

## RESEARCH ARTICLE

# Blood DNA methylation signature for incident dementia: Evidence from longitudinal cohorts

Wei Zhang<sup>1</sup> | Juan I. Young<sup>2,3</sup> | Lissette Gomez<sup>3</sup> | Michael A. Schmidt<sup>2,3</sup> |  
David Lukacsovich<sup>1</sup> | Brian W. Kunkle<sup>2,3</sup> | X. Steven Chen<sup>1,4</sup> | Eden R. Martin<sup>2,3</sup> |  
Lily Wang<sup>1,2,3,4</sup>

<sup>1</sup>Division of Biostatistics, Department of Public Health Sciences, Miller School of Medicine, University of Miami, Miami, Florida, USA

<sup>2</sup>Dr. John T. Macdonald Foundation Department of Human Genetics, Miller School of Medicine, University of Miami, Miami, Florida, USA

<sup>3</sup>John P. Hussman Institute for Human Genomics, Miller School of Medicine, University of Miami, Miami, Florida, USA

<sup>4</sup>Sylvester Comprehensive Cancer Center, Miller School of Medicine, University of Miami, Miami, Florida, USA

## Correspondence

Lily Wang, Soffer Clinical Research Ctr,  
University of Miami Miller School of Medicine,  
1120 NW 14th St, Miami, FL 33136-2107,  
USA.  
Email: [lily.wang@gmail.com](mailto:lily.wang@gmail.com)

Data used in the preparation of this article were obtained from the Alzheimer's Disease Neuroimaging Initiative (ADNI) database (<http://adni.loni.usc.edu>). As such, the ADNI investigators contributed to the design and implementation of ADNI and/or provided data but did not participate in the analysis or writing of this report. A complete listing of ADNI investigators is available at: [http://adni.loni.usc.edu/wp-content/uploads/how\\_to\\_apply/ADNI\\_Acknowledgement\\_List.pdf](http://adni.loni.usc.edu/wp-content/uploads/how_to_apply/ADNI_Acknowledgement_List.pdf)

## Funding information

US National Institutes of Health; National Institute on Aging, Grant/Award Number: R01AG062634; National Institute of Neurological Disorders and Stroke, Grant/Award Numbers: RF1NS128145, R61NS135587

## Abstract

**INTRODUCTION:** Distinguishing between molecular changes that precede dementia onset and those resulting from the disease is challenging with cross-sectional studies.

**METHODS:** We studied blood DNA methylation (DNAm) differences and incident dementia in two large longitudinal cohorts: the Offspring cohort of the Framingham Heart Study (FHS) and the Alzheimer's Disease Neuroimaging Initiative (ADNI) study. We analyzed blood DNAm samples from > 1000 cognitively unimpaired subjects.

**RESULTS:** Meta-analysis identified 44 CpGs and 44 differentially methylated regions consistently associated with time to dementia in both cohorts. Our integrative analysis identified early processes in dementia, such as immune responses and metabolic dysfunction. Furthermore, we developed a methylation-based risk score, which successfully predicted future cognitive decline in an independent validation set, even after accounting for age, sex, apolipoprotein E ε4, years of education, baseline diagnosis, and baseline Mini-Mental State Examination score.

**DISCUSSION:** DNAm offers a promising source as a biomarker for dementia risk assessment.

## KEYWORDS

dementia, DNA methylation, longitudinal study

## Highlights

- Blood DNA methylation (DNAm) differences at individual CpGs and differentially methylated regions are significantly associated with incident dementia.

This is an open access article under the terms of the [Creative Commons Attribution-NonCommercial](https://creativecommons.org/licenses/by-nc/4.0/) License, which permits use, distribution and reproduction in any medium, provided the original work is properly cited and is not used for commercial purposes.

© 2025 The Author(s). *Alzheimer's & Dementia* published by Wiley Periodicals LLC on behalf of Alzheimer's Association.

- Pathway analysis revealed DNAm differences associated with incident dementia are significantly enriched in biological pathways involved in immune responses and metabolic processes.
- Out-of-sample validation analysis demonstrated that a methylation-based risk score successfully predicted future cognitive decline in an independent dataset, even after accounting for age, sex, apolipoprotein E  $\epsilon$ 4, years of education, baseline diagnosis, and baseline Mini-Mental State Examination score.

## 1 | BACKGROUND

Alzheimer's disease and related dementias (ADRD) are a major public health problem with a substantial economic burden.<sup>1</sup> ADRD currently affects 8.1 to 10.8 million Americans in the United States,<sup>2</sup> and this number is projected to rise as the population ages. The escalating health-care demands of ADRD underscore the critical need for effective prevention, early diagnosis, and management approaches.

Given the difficulty in halting neurodegenerative processes once they begin, it is imperative to develop biomarkers that could identify individuals at high risk for developing Alzheimer's disease (AD) while they are still cognitively unimpaired (CU). Such biomarkers can facilitate personalized medicine and the implementation of preventive lifestyle interventions, potentially delaying the onset of dementia. Recent studies showed that delaying the onset of dementia by only 1 year in the 70- to 74-year-old group could reduce prevalence by >10%.<sup>3</sup>

DNA methylation (DNAm) is an epigenetic mechanism influenced by both genetics and environment. We and others have shown that DNAm is integrally involved in AD dementia.<sup>4–11</sup> Moreover, several recent studies demonstrated DNAm differences could be detected in blood samples of AD subjects.<sup>12–17</sup> In particular, our recent analysis of two large clinical AD datasets (Alzheimer's Disease Neuroimaging Initiative [ADNI] and Australian Imaging Biomarkers and Lifestyle study) revealed a number of blood DNAm differences consistently associated with AD diagnosis in both cohorts.<sup>7</sup>

To develop biomarkers that can assess individual risk for dementia, it is important to distinguish between DNAm changes that precede dementia onset and those that result from the disease. To date, most studies of DNAm in dementia have used a cross-sectional design,<sup>6,7,16–18</sup> with only a few using the longitudinal design. Encouragingly, two recent longitudinal studies detected DNAm changes in the blood several years before the onset of dementia symptoms.<sup>19–22</sup> However, these studies were limited by their small sample sizes.

Here we studied DNAm and incident dementia by meta-analyzing two large longitudinal datasets from the Framingham Heart Study (FHS) and the ADNI studies, with a total of > 1000 samples from independent subjects, free of dementia or mild cognitive impairment (MCI) at blood sample collection. All samples included in this meta-analysis were measured using the same Infinium MethylationEPIC Beadchip platform, and each dataset was analyzed using a uniform analytical pipeline. We identified CpGs and differentially methylated

regions (DMRs) consistently associated with incident dementia in both cohorts. Moreover, we also performed comparative analysis incorporating results from integrative analysis of DNAm in the blood with gene expression, genetic variants, and brain DNAm. These analyses, along with gene set enrichment analysis, highlighted DNAm differences associated with immune responses and metabolic dysfunction in dementia. In addition to corroborating findings from previous studies using cross-sectional design, our analysis also nominated a number of novel DNAm differences, emphasizing the importance of using a longitudinal design to identify DNAm differences with a temporal relationship to the disease. Importantly, we developed a methylation risk score (MRS) for dementia using the FHS dataset and successfully validated it through out-of-sample testing on the ADNI dataset, demonstrating DNAm is a plausible source of predictive biomarkers for dementia.

## 2 | METHODS

### 2.1 | Study datasets for meta-analysis

The FHS is a community-based transgenerational study that investigates the development of cardiovascular disease in Framingham, Massachusetts.<sup>23</sup> In the FHS, the Offspring cohort included subjects from the second generation and their spouses. Blood samples were collected from the FHS Offspring cohort at Exam 9 (denoted FHS9 hereafter) which took place between 2011 and 2014. We included samples from 907 self-reported non-Hispanic White subjects who were free of dementia at FHS9.

In the FHS, participants undergo a Mini-Mental State Examination (MMSE) at each exam cycle, and they completed a 45 minute neuropsychological test every 5 to 6 years since 1999. If participants are flagged for possible cognitive impairment based on these assessments, they are invited for additional, annual neurological and neuropsychological evaluations. If two consecutive annual evaluations show improvement, participants return to the regular follow-up schedule.<sup>24</sup> Details of dementia surveillance in the FHS were previously described in Satizabal et al.<sup>24</sup> A dementia review panel assesses all potential cases, and the diagnosis of dementia is based on Diagnostic and Statistical Manual of Mental Disorders, fourth edition (DSM-IV) criteria. DNAm data and dementia ascertainment were obtained from the dbGap database (accessions: phs000974.v5.p4 and pht010750.v2.p14).

The ADNI is a longitudinal study designed to study the progression of AD.<sup>25</sup> For our analysis, we selected the earliest visit with available DNAm data for each subject, and additionally required that they were CU at that time. This resulted in a dataset of 216 self-reported non-Hispanic White subjects.<sup>26</sup> These subjects were followed approximately every 6 months, which provides valuable information on disease progression. DNAm data and the dementia status of the subjects were obtained from the ADNI study website (adni.loni.usc.edu).

The endpoint of this study is dementia onset. The follow-up period was from the time of blood sample collection for DNAm measurement to the time of dementia onset. Follow-up was censored at the time of loss to follow-up, non-dementia death, or the final day of study follow-up.

## 2.2 | Preprocessing of DNAm data

DNAm samples from both FHS9 and ADNI were measured using the same Illumina HumanMethylation EPIC v1 bead chips. Table S1 in supporting information shows the number of CpGs and samples at each quality control (QC) step. The FHS9 and ADNI datasets were preprocessed separately. For each dataset, the QC of probes involved several steps. First, we selected probes with a detection  $p$  value  $< 0.01$  in  $\geq 90\%$  of the samples. A small  $p$  value indicates a significant difference between the signals in the probes and the background noise. Next, we selected probes that start with "cg," and using the function `rmSNPandCH` from the `DMRcate` R package, we removed probes that are located on X and Y chromosomes, are cross-reactive,<sup>27</sup> or located close to single nucleotide polymorphism (SNPs; i.e., an SNP with minor allele frequency [MAF]  $\geq 0.01$  was present in the last five base pairs of the probe).

For QC of the samples, we first removed samples with bisulfite conversion rate  $< 85\%$ , as well as samples for which the DNAm predicted sex status differed from the recorded sex status. The sex prediction was performed using the `getSex` function from the `minfi` R package. In addition, we performed principal component analysis (PCA) using the 50,000 most variable CpGs to identify outliers. Samples outside the range of  $\pm 3$  standard deviations from the mean of first principal component (PC1) and second principal component (PC2) were excluded.

The quality-controlled data were next normalized using the `dasen` method, as implemented in the `watermelon` R package.<sup>28</sup> Immune cell type proportions (B lymphocytes, natural killer cells, CD4+ T cells, CD8+ T cells, monocytes, neutrophils, and eosinophils) were estimated using the `EpiDISH` R package.<sup>29</sup> As in previous blood-based DNAm studies,<sup>6,7,30</sup> granulocyte proportions were computed as the sum of neutrophil and eosinophil proportions because both neutrophils and eosinophils are classified as granular leukocytes. To correct batch effects from methylation plates, we used the `BEEclear` R package.<sup>31</sup>

Figures S1 and S2 in supporting information show that the PC1 of methylation beta values was not significantly associated with covariates including follow-up duration, age, sex, education, and smoking history of the subjects in ADNI and FHS9 datasets, with the excep-

## RESEARCH IN CONTEXT

- Systematic review:** The authors conducted a comprehensive search and review of studies investigating the relationship between blood DNA methylation (DNAm) and dementia. This review revealed that most studies have used cross-sectional design, with only a few using longitudinal design. However, the longitudinal studies were limited by their small sample sizes.
- Interpretation:** Our findings underscore DNAm as an early biomarker for dementia, highlighting immune responses and metabolic dysfunction as key early processes. Our out-of-sample validation demonstrated that methylation-based risk scores predicted future cognitive decline in an independent dataset, even after accounting for covariate variables, supporting blood DNAm as a potential objective biomarker for identifying individuals at higher risk for dementia.
- Future directions:** Future research should aim to validate these DNAm markers in larger, more diverse cohorts. Developing precise methylation risk scores could facilitate early detection and personalized interventions, ultimately leading to the delay or prevention of dementia onset.

tion that PC1 was significantly higher in males in the FHS9 dataset. All subsequent analyses were adjusted for sex along with other potential confounding factors.

## 2.3 | Association of DNAm at individual CpGs with dementia

To evaluate the relationship between incident dementia and DNAm, we conducted Cox proportional regression analyses on both FHS and ADNI datasets separately, via the `coxph` function in the `survival` R package. For the FHS dataset, we used the model: `Surv (follow-up time, status) ~ methylation.beta + age + sex + immune cell-type proportions (B, NK, CD4T, Mono, Gran)` where status indicates whether incident dementia occurred (1 = event occurred, 0 = censored; Model 1). For the ADNI dataset, given the smaller sample size, we only included the first two principal components (PCs) of the immune cell-type proportions, which explained 90.0% variances in estimated immune cell-type proportions. Specifically, we fitted the model `Surv (follow-up time, status) ~ methylation.beta + age + sex + PC1 + PC2`.

## 2.4 | Inflation assessment and correction

Genomic inflation factors (lambda values) were estimated using both the conventional approach<sup>32</sup> and the `bacon` method,<sup>33</sup> which was pro-

posed specifically for epigenome-wide association studies. For the FHS and ADNI datasets, the estimated bias was  $-0.009$  and  $0.041$ , respectively. For the estimated inflation, the lambda values ( $\lambda$ ) using the conventional approach were  $1.424$  and  $1.005$ , while the lambda values based on the bacon approach ( $\lambda_{\text{bacon}}$ ) were  $1.176$  and  $0.986$  for the FHS and ADNI datasets, respectively (Table S2 in supporting information).

We next applied genomic correction using the bacon method,<sup>33</sup> as implemented in the bacon R package, to obtain bacon-corrected effect sizes, standard errors, and  $p$  values for each dataset. After bacon correction, the estimated biases were  $4.78 \times 10^{-4}$  and  $-6.18 \times 10^{-4}$ , and the estimated inflation factors were  $\lambda = 1.03$  and  $1.029$ , and  $\lambda_{\text{bacon}} = 1.01$  and  $1.00$  for the FHS and ADNI datasets, respectively.

## 2.5 | Meta-analyses

To meta-analyze individual CpG results across both the FHS9 and ADNI datasets, we used the inverse-variance weighted fixed-effects model, implemented in the meta R package. As demonstrated by Rice et al., the fixed effects model can be interpreted as a weighted average of study-specific effects, regardless of whether the true study-specific effects are heterogeneous.<sup>34</sup> The methylation beta values were rescaled into  $z$  scores so that the estimated hazard ratios (HRs) correspond to an increase in dementia risk associated with a one standard deviation increase in beta values. To correct for multiple comparisons, we computed the false discovery rate (FDR). We considered CpGs with an  $\text{FDR} < 5\%$  in meta-analyses of the FHS9 and ADNI datasets, with a consistent direction of change in estimated effect sizes, and a nominal  $p$  value  $< 0.05$  in both datasets as statistically significant.

## 2.6 | DMR analysis

For region-based meta-analyses, we used the comb-p method.<sup>35</sup> Briefly, comb-p takes single CpG  $p$  values and locations of the CpG sites to scan the genome for regions enriched with a series of adjacent low  $p$  values. In our analysis, we used  $p$  values from the meta-analysis of the FHS9 and ADNI datasets as input for comb-p. We used parameter settings with  $-\text{seed } 0.05$  and  $-\text{dist } 750$  (a  $p$  value of  $0.05$  is required to start a region and extend the region if another  $p$  value was within  $750$  base pairs), which were shown to have optimal statistical properties in our previous comprehensive assessment of the comb-p software.<sup>36</sup> As comb-p uses the Sidak method to account for multiple comparisons, we selected DMRs with Sidak  $p$  values  $< 0.05$ . To help reduce false positives, we imposed two additional criteria in our final selection of DMRs: (1) the DMR also has a nominal  $p$  value  $< 1 \times 10^{-5}$  and (2) all the CpGs within the DMR have a consistent direction of change in estimated effect sizes in the meta-analysis.

## 2.7 | Functional annotation of significant methylation associations

The significant methylation at individual CpGs and DMRs were annotated using both the Illumina (University of California Santa Cruz) gene annotation and Genomic Regions Enrichment of Annotations Tool (GREAT) software,<sup>37</sup> which associates genomic regions with target genes. To assess the overlap between our significant CpGs and DMRs (CpG or DMR location  $\pm 250$  bp) with enhancers, we used enhancer gene maps generated from 131 human cell types and tissues described in Nasser et al.<sup>38</sup> Specifically, we selected enhancer-gene pairs with "positive" predictions from the Activity-by-Contact (ABC) model, which included only expressed target genes, did not include promoter elements, and had an ABC score  $> 0.015$ . In addition, we also required that the enhancer-gene pairs be identified in cell lines relevant to this study.

## 2.8 | Pathway analysis

To identify biological pathways enriched with significant DNAm differences, we used the methylRRA function in the methylGSA R package,<sup>39</sup> which used  $p$  values from the meta-analysis of FHS9 and ADNI datasets as input. Briefly, methylGSA first computes a gene-wise  $p$  value by aggregating  $p$  values from multiple CpGs mapped to each gene. Next, the different number of CpGs on each gene is adjusted by Bonferroni correction. Finally, a gene set enrichment analysis<sup>40</sup> (in pre-rank analysis mode) is performed to identify pathways enriched with significant CpGs. We analyzed pathways in the Kyoto Encyclopedia of Genes and Genomes (KEGG) and Reactome databases. Pathways with  $\text{FDR} < 0.05$  were considered statistically significant.

## 2.9 | Integrative analyses with gene expression, genetic variants, and brain-to-blood correlations

To evaluate the effect of DNAm on the expression of nearby genes, we overlapped our dementia-associated CpGs, including both significant individual CpGs and those located within DMRs, with expression quantitative trait methylation (eQTM) analysis results in Tables S2 and S3 of Yao et al.<sup>41</sup>

For correlation and overlap with genetic susceptibility loci, We searched for methylation quantitative trait loci (mQTLs) in the blood using the GoDMC database.<sup>42</sup> To select significant blood mQTLs in GoDMC, we used the same criteria as the original study,<sup>42</sup> that is, considering a cis  $p$  value  $< 10^{-8}$  and a trans  $p$  value  $< 10^{-14}$  as significant. The genome-wide summary statistics for genetic variants associated with dementia described in Bellenguez et al.<sup>43</sup> were obtained from the European Bioinformatics Institute GWAS Catalog under accession no. GCST90027158. Colocalization analysis was performed using the coloc R package.

To assess the correlation of dementia-associated CpG and DMR methylation levels in blood and brain samples, we used the London dataset, which consisted of 69 samples with matched prefrontal cortex and blood samples.<sup>44</sup> We assessed the association of brain and blood methylation levels at dementia-associated CpGs using both an unadjusted correlation analysis with methylation beta values ( $r_{\text{beta}}$ ), and an adjusted correlation analysis using methylation residuals ( $r_{\text{resid}}$ ), in which we removed the effect of estimated neuron proportions in brain samples (or estimated immune cell-type proportions in blood samples), methylation plates, age at death for brain samples (or age at blood draw for blood samples), and sex from DNAm  $M$  values.

## 2.10 | Sensitivity analyses

In the first sensitivity analysis, we evaluated if dementia risk factors would likely confound the DNAm to dementia associations we observed. To this end, we first performed regression analysis to assess the association between dementia-associated CpGs (both significant individual CpGs and those located in DMRs) and dementia risk factors collected by the FHS, including diabetes status, blood pressure, years of education, obesity, and smoking. Specifically, for each risk factor and each CpG, we fitted the model  $\text{methylation.m.value} \sim \text{risk factor} + \text{age} + \text{sex} + \text{cell type proportions (B, NK, CD4T, Mono, Gran)}$ . A risk factor is considered significantly associated with a CpG if its  $p$  value is  $<0.05$  in the above model.

Next, the confounding effects of these significant risk factors for the dementia-associated CpGs were evaluated by fitting the Cox proportional regression model that expanded Model 1 above by additionally including the significant risk factor:  $\text{Surv(incident dementia, follow-up time)} \sim \text{methylation.beta} + \text{risk factor} + \text{age} + \text{sex} + \text{immune cell-type proportions (B, NK, CD4T, Mono, Gran)}$ .

In the second sensitivity analysis, to evaluate the impact of family structure in the discovery of significant CpGs, we computed the intraclass correlation coefficient (ICC) for dementia-associated CpGs, by fitting a random effects model  $\text{methylation m-value} \sim \text{random (family)}$  to the FHS9 data for each CpG. The ICC was then estimated by  $\frac{\sigma_u^2}{\sigma_u^2 + \sigma_e^2}$  where  $\sigma_u^2$  is estimated variance component for family random effects and  $\sigma_e^2$  is the residual error. This analysis was implemented using the `lmer` function in the `lme4` R package.

We also compared the results of Model 1 to a model that accounts for family relationships in the Cox regression model using a kinship matrix. To this end, we first computed the kinship matrix using the R package `kinship2` based on the pedigree information in the dbGap dataset (accession: pht000183.v13.p14). Next, for each dementia-associated CpG, we fitted a mixed-effects Cox regression model with a random intercept, adjusting for the same covariates as in Model 1 above in the analysis of the FHS9 dataset. The variance-covariance matrix is determined using twice the value of the kinship matrix.<sup>45</sup> The mixed-effects Cox models were implemented using the `coxme` R package.

Additionally, the `coMethDMR`<sup>46</sup> software was used to evaluate the robustness of genomic regions defined by the 44 DMRs identified by `comb-p` for their association with time-to-incident dementia. First, `coMethDMR` selected co-methylated sub-regions within for each region. We then summarized methylation beta values within these co-methylated sub-regions using medians and tested them against time to incident dementia. In the same way as in single CpG analyses, we adjusted for potential confounding factors, including age, sex, and blood cell-type composition. The dataset specific  $p$  values for each genomic region were then combined across FHS9 and ADNI datasets using an inverse-variance weighted fixed effects meta-analysis model. DMRs with an FDR of  $< 5\%$  were considered significant.

Finally, in the last sensitivity analysis, to identify cases with dementia or MCI due to AD in the ADNI dataset, we use the variables `DXMDUE` and `DXDUE` in the `DXSUM` table. Similarly, we used the variable `AD_STATUS` in the FHS9 dataset to identify AD cases.

## 2.11 | Validation using independent datasets

To compare our results to previous findings, we searched dementia-associated CpGs (both significant individual CpGs and those located in DMRs) using the CpG Query tool in the DNA Methylation in Aging and Methylation in AD (MIAMI-AD) database. For input on phenotype, we selected "AD biomarker," "AD neuropathology," "dementia clinical diagnosis."

## 2.12 | Out-of-sample validation of MRS

First, we selected CpGs that achieved  $p$  value  $< 10^{-5}$  using the model  $\text{Surv (follow-up time, status)} \sim \text{methylation.beta} + \text{age} + \text{sex} + \text{immune cell-type proportions (B, NK, CD4T, Mono, Gran)}$  where status indicates whether incident dementia occurred (1 = event occurred, 0 = censored) in the FHS9 dataset. To estimate CpG weights, we applied ridge regression using the `glmnet` R package to the FHS9 dataset. The model parameters  $\lambda$  was optimized via 5-fold cross-validation based on the Harrell C index. After tuning the model, the final model was fitted with  $\lambda = \text{lambda.1se}$ , that is, the value of  $\lambda$  that gives the most regularized model such that the cross-validated C index is within one standard error of the maximum.

Next, we performed an out-of-sample validation using the ADNI dataset. For each subject at baseline, the MRS was computed by summing the methylation  $M$  values for the 151 CpGs weighted by coefficients estimated from the ridge regression model described above. We then performed Cox regression analyses on the ADNI dataset to evaluate the association between baseline MRS and disease progression. This analysis was performed using the `coxph` function in the `survival` R package. Disease progression was defined as the conversion from CU to MCI or dementia, and from MCI to dementia. The model was adjusted for multiple covariates:  $\text{Surv (Conversion event, follow-up time)} \sim \text{MRS} + \text{age} + \text{sex} + \text{apolipoprotein E (APOE) } \epsilon 4 \text{ status} +$



**TABLE 1** Characteristics of subjects included in the meta-analysis of the FHS9 and ADNI cohorts.

Characteristics	Framingham Heart Study Offspring Cohort at Exam 9				ADNI (earliest visit with DNA methylation data)			
	All (n = 907)	Dementia (n = 42)	Control (n = 865)	p value	All (n = 216)	Dementia (n = 18)	Control (n = 198)	p value
Follow-up period in years								
Average (SD)	4.98 (2.33)	3.06 (1.84)	5.07 (2.31)	$2.24 \times 10^{-8}$	5.97 (3.00)	6.42 (2.72)	5.92 (3.03)	0.513
Age, average (SD)	72.03 (8.18)	79.26 (5.96)	71.68 (8.12)	$2.77 \times 10^{-9}$	76.73 (6.62)	74.92 (3.98)	76.63 (6.75)	0.368
Sex, n (%)								
Female	496 (54.69)	20 (47.62)	476 (55.03)	0.428	108 (50.00)	10 (55.56)	98 (49.50)	0.806
Male	411 (45.31)	22 (52.38)	389 (44.07)		108 (50.00)	8 (44.44)	100 (51.50)	
Mean education year, average (SD)	14.38 (2.53)	13.84 (2.39)	14.41 (2.54)	0.317	16.36 (2.67)	16.11 (2.70)	16.38 (2.67)	0.522
Smoking history, n (%)								
Yes	549 (60.60)	29 (69.05)	520 (60.19)	0.332	92 (42.59)	8 (44.44)	84 (42.42)	1.000

Note: Dementia subjects are defined as those who developed dementia during the follow-up period; control subjects are those who did not develop dementia during the observation period or were lost to follow-up.

Abbreviations: ADNI, Alzheimer's Disease Neuroimaging Initiative; FHS9, Framingham Heart Study Exam 9; SD, standard deviation.

years of education + baseline diagnosis + baseline MMSE score. Furthermore, we stratified the samples into four groups based on quartiles of their baseline MRS scores and visualized the conversion probabilities for the subjects in the first and last quartiles, after adjusting for covariate variables age, sex, APOE ε4 status, years of education, baseline diagnosis, and baseline MMSE score. The adjusted Kaplan–Meier curves were graphed using the ggadjustedcurves function from the survminer R package.

### 2.13 | Data and code availability

The genome-wide summary statistics have been deposited to the MIAMI-AD database (<https://miami-ad.org/>). The scripts for the analyses performed in this study are available at <https://github.com/TransBioInfoLab/blood-dnam-and-incident-dementia>

## 3 | RESULTS

### 3.1 | Study cohorts

Our meta-analysis included a total of 1123 DNAm samples (measured using Illumina EPIC arrays), generated from blood samples of 907 Offspring cohort participants (496 females, 411 males) in the FHS9 and 216 participants (108 females, 108 males) in the ADNI study (Table 1), who were free of dementia or MCI diagnosis at blood sample collection.

In the FHS, the mean age of the subjects at blood collection during FHS9 was  $72.03 \pm 8.18$  years. The subjects in FHS9 were followed up to 7.72 years after exam 9, with an average follow-up of  $4.98 \pm 2.33$  years, and 42 subjects developed dementia during this period. In particular, for those who did not develop dementia by the end of the observation period in 2018, the average follow-up duration was  $5.07 \pm 2.31$  years (Table 1, Figure S3 in supporting information).

In the ADNI, the mean age of the participants at the time of sample collection was  $76.73 \pm 6.62$  years. These subjects were followed for up to 11.11 years, with an average follow-up of  $5.97 \pm 3.00$  years, and 18 subjects developed dementia during this period. For those who did not develop dementia by the end of the observation period, the average follow-up duration was  $5.92 \pm 3.03$  years (Table 4, Figure S4 in supporting information). The percentages of non-smokers in FHS9 and ADNI were 39.40% and 57.41%, respectively. Subjects in both cohorts are highly educated, with an average of 14.38 years of education in FHS9 and 16.36 years in ADNI.

### 3.2 | Blood DNAm differences at individual CpGs and DMRs are significantly associated with incident dementia

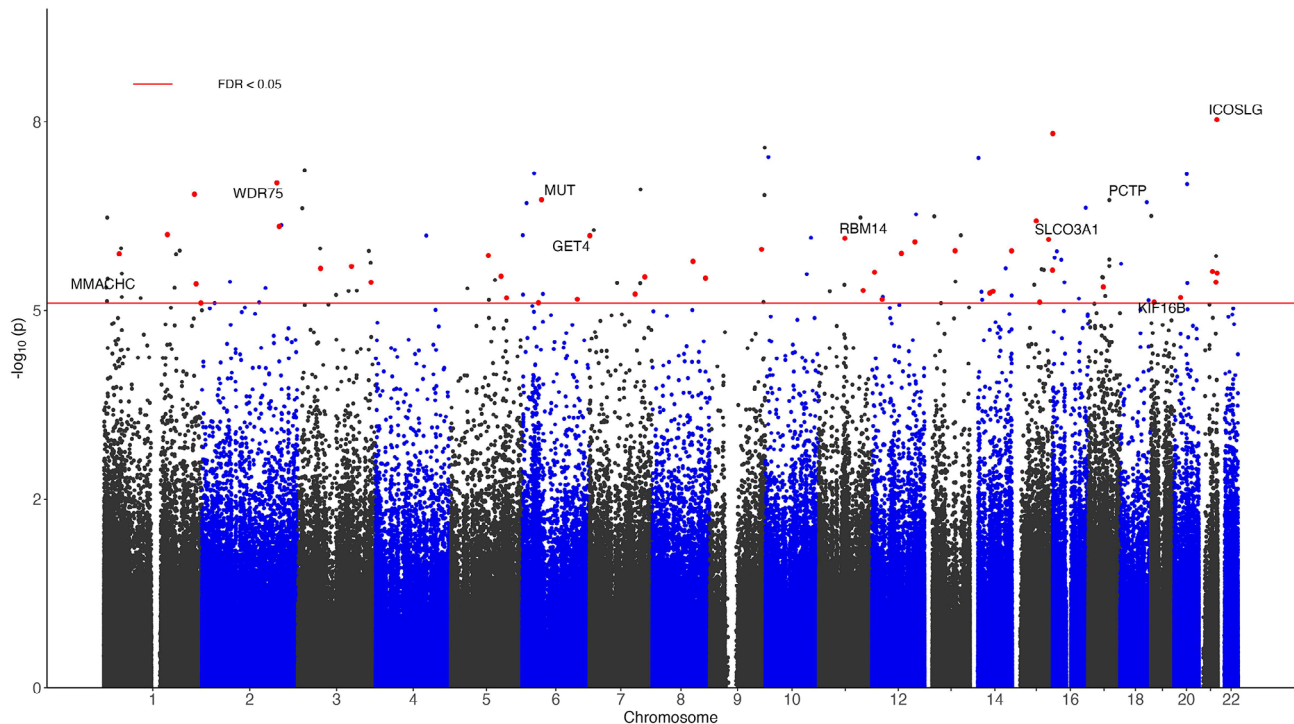
After adjusting for age, sex, and immune cell type proportions, and correcting batch effects and genomic inflation (see the Methods section), we identified 44 CpGs with a consistent direction of change in both FHS9 and ADNI datasets, a nominal  $p$  value  $< 0.05$  in each individual dataset and an FDR  $< 0.05$  in inverse-variance fixed-effects meta-analysis of the FHS9 and ADNI datasets (Figure 1, Table 2, and Table S3 and Figure S5 in supporting information). These results remain robust in models that additionally included dementia risk factors and accounted for family structure in the FHS (see details below). For these 44 significant CpGs, the HRs associated with one standard deviation change in methylation beta values ranged from 0.456 to 3.948 in the FHS9 cohort, 0.343 to 2.577 in the ADNI cohort, and 0.428 to 3.063 in the meta-analysis. Approximately half of the significant CpGs (21 CpGs) showed hypermethylation associated with an increased risk of dementia. Approximately half of these CpGs (20 CpGs) are located in CpG islands or shores. Additionally, 19 CpGs (43.18%) are in promoter regions within 2 kb of the transcription start site, which is significantly higher than the overall proportion of CpGs in

TABLE 2 Top 10 most significant CpGs associated with incident dementia in the meta-analysis of blood samples in ADNI and FHS9 datasets.

CpG	Chr	Position	Meta-analysis of FHS9 and ADNI cohorts					FHS9					ADNI				
			Estimate	StdErr	HR	p value	FDR	Direction	Estimate	StdErr	HR	p value	Estimate	StdErr	HR	p value	GREAT_annotation
cg24327461	chr21	45,661,066	0.369	0.067	1.446	2.97E-08	1.48E-02	++	0.360	0.071	1.433	3.61E-07	0.439	0.197	1.551	2.57E-02	ICOSLG (–239)
cg06059043	chr16	559,311	–0.379	0.069	0.684	4.54E-08	1.48E-02	–	–0.421	0.094	0.656	8.08E-06	–0.330	0.102	0.719	1.25E-03	CAPN15 (–18545); RAB11FIP3 (+83693)
cg13259821	chr2	190,305,888	0.430	0.083	1.537	2.04E-07	1.64E-02	++	0.408	0.088	1.504	3.91E-06	0.584	0.235	1.793	1.29E-02	WDR75 (–271)
cg19011876	chr1	230,344,452	–0.686	0.134	0.504	2.87E-07	1.72E-02	–	–0.644	0.165	0.525	9.19E-05	–0.766	0.229	0.465	8.08E-04	GALNT2 (+141497); PGBD5 (+168939)
cg07931783	chr6	49,431,133	0.581	0.114	1.788	3.42E-07	1.72E-02	++	0.546	0.125	1.727	1.30E-05	0.747	0.274	2.111	6.42E-03	MUT (–230); CENPQ (+43)
cg27044052	chr15	61,055,914	–0.712	0.143	0.491	6.51E-07	2.02E-02	–	–0.786	0.177	0.456	9.23E-06	–0.573	0.242	0.564	1.80E-02	RORA (–136253)
cg09015682	chr2	196,363,897	–0.629	0.127	0.533	7.70E-07	2.21E-02	–	–0.638	0.161	0.529	7.22E-05	–0.613	0.208	0.542	3.20E-03	SLC39A10 (–157574)
cg06059345	chr1	161,654,727	–0.293	0.060	0.746	9.89E-07	2.40E-02	–	–0.277	0.062	0.758	7.01E-06	–0.566	0.254	0.568	2.56E-02	FCRLA (–22035); FCGR2B (+21777)
cg04220579	chr7	915,756	0.359	0.073	1.431	1.02E-06	2.40E-02	++	0.363	0.087	1.437	2.99E-05	0.348	0.137	1.417	1.09E-02	GET4 (–433)
cg16838301	chr11	66,384,437	0.396	0.081	1.486	1.11E-06	2.46E-02	++	0.350	0.089	1.419	7.72E-05	0.643	0.205	1.902	1.72E-03	RBM14-RBM4 (+341); RBM14 (+385)

Note: Inverse-variance weighted fixed-effects meta-analysis models were used to combine cohort-specific results from Cox regression models that included covariate variables age, sex, and immune cell-type proportions. HR describe changes in risk of dementia associated with a one standard deviation increase in methylation beta values after adjusting for covariate variables. We corrected batch effects using the BEclear R package, and corrected genomic inflation using the bacon R package. Direction indicates hypermethylation (+) or hypomethylation (–) of the CpG associated with increased risk of dementia in FHS9 and ADNI datasets. In GREAT annotation, the numbers in parentheses indicate the distance from the TSS.

Abbreviations: ADNI, Alzheimer’s Disease Neuroimaging Initiative; FDR, false discovery rate; FHS9, Framingham Heart Study Exam 9; GREAT, Genomic Regions Enrichment of Annotations Tool; HR, hazard ratio; TSS, transcription start site.



**FIGURE 1** Manhattan plot of significant DNA methylation differences associated with incident dementia in meta-analysis of FHS9 and ADNI datasets. The x axis indicates chromosome number. The y axis shows  $\log_{10}(p)$  value of meta-analysis, with red line indicating a 5% FDR. The genes with promoter regions containing the top 10 most significant CpGs are highlighted. The red dots correspond to the 44 CpGs with a consistent direction of change in both FHS9 and ADNI datasets, a nominal  $p$  value  $< 0.05$  in both datasets, and an FDR  $< 0.05$  in meta-analyses of the FHS9 and ADNI datasets. ADNI, Alzheimer's Disease Neuroimaging Initiative; FDR, false discovery rate; FHS9, Framingham Heart Study Exam 9.

promoter regions (27.65%;  $p$  value = 0.0276; Figure S6 in supporting information).

Using meta-analysis  $p$  values for individual CpGs as input, comb-p<sup>35</sup> software identified 44 DMRs, which had a nominal  $p$  value  $< 1 \times 10^{-5}$ , Sidak adjusted  $p$  value  $< 0.05$ , and all the CpGs within the DMR have a consistent direction of change in estimated effect sizes in the meta-analysis (Table 3, Table S4 in supporting information). The number of CpGs in these DMRs ranged from 3 to 12. Among these DMRs, the majority showed hypermethylation associated with increased risk of dementia (35 DMRs), are located in CpG islands or shore (23 DMRs), or the promoter region (31 DMRs). Interestingly, among the significant individual CpGs and DMRs, 10 CpGs and 15 DMRs were also located in enhancer regions (Tables S3 and S4), which are regulatory DNA sequences that transcription factors bind to to activate gene expression.<sup>38,47</sup>

### 3.3 | Pathway analysis revealed DNAm differences associated with risk of dementia are enriched in biological pathways involved in immune responses and metabolic processes

To better understand biological pathways enriched with significant DNAm differences, we next performed pathway analysis using the methylGSA software.<sup>39</sup> At 5% FDR, we identified 28 KEGG pathways

and 26 Reactome pathways (Figure 2 and Table S5 in supporting information). Notably, a number of these significant pathways highlighted the central role of neuroinflammation processes in dementia, such as B cell receptor signaling, chemokine signaling, leukocyte transendothelial migration, interleukin-1 signaling, and Toll-like receptor cascades pathways. In addition, several other significant pathways are involved in metabolic processes, including glucose and lipid metabolism, dysfunction of which are major risk factors for dementia.<sup>48,49</sup> These significant pathways included glycolysis/gluconeogenesis, insulin signaling, and steroid biosynthesis.

### 3.4 | Correlation of significant DNAm with expression of nearby genes and brain DNAm levels

To better understand the functional role of the significant DMRs and CpGs, we performed several comparative analyses. We first overlapped our significant DNAm differences with previously established DNAm to RNA associations (i.e., eQTM) which was identified using matched DNAm and gene expression data from the FHS.<sup>41</sup> Among the 44 significant individual CpGs and those within the 44 DMRs, we found 13 and 15 CpGs significantly correlated with target gene expression in cis (i.e., within 500k bp of the CpG) or trans, respectively (Table S6 in supporting information). Notably, all the CpGs with cis associations are negatively correlated with their target gene expressions. Among them,



**TABLE 3** Top 10 most significant DMRs associated with incident dementia.

DMR	n_probes	p value	Sidak adjusted p value	Direction	GREAT_annotation
chr17:53828263-53828931	11	3.58E-22	4.16E-19	+++++	PCTP (+257)
chr21:26934178-26934886	8	4.52E-20	4.95E-17	+++++	MRPL39 (+45297)
chr1:45965449-45966116	10	7.45E-15	8.66E-12	+++++	MMACHC (+57)
chr20:16555475-16555995	5	1.44E-11	2.15E-08	+++++	KIF16B (-1657)
chr12:44152509-44152941	10	1.12E-10	2.01E-07	+++++	PUS7L (-164);IRAK4 (-33)
chr7:915756-915832	3	7.32E-11	7.48E-07	+++	GET4 (-395)
chr19:33182526-33182835	5	3.86E-09	9.69E-06	+++++	NUDT19 (-187)
chr11:67417958-67418366	8	7.26E-09	1.38E-05	---	ACY3 (-32)
chr15:92396240-92396450	3	6.02E-09	2.23E-05	+++	SLCO3A1 (-580)
chr21:30391563-30391823	5	7.74E-09	2.31E-05	+++++	RWDD2B (+6)

Note: Direction indicates directions of CpGs within each DMR in the meta-analysis of FHS9 and ADNI datasets, with hypermethylation (+) or hypomethylation (-) associated with increased risk of dementia. In GREAT annotation, the numbers in parentheses indicate the distance from the TSS.

Abbreviations: ADNI, Alzheimer's Disease Neuroimaging Initiative; DMR, differentially methylated region; FHS9, Framingham Heart Study Exam 9; GREAT, Genomic Regions Enrichment of Annotations; TSS, transcription start site.

six CpGs in the promoter regions of the *KIF16B* gene are significantly associated with its gene expression.

As dementia is a brain disorder, we also sought to prioritize methylation differences with a consistent direction of change in both blood and brain. To this end, we computed Spearman rank correlations between DNAm levels in the brain and blood using the London dataset,<sup>9</sup> which included matched DNAm samples measured on *post mortem* brain and *ante mortem* blood samples of 69 subjects.<sup>44</sup> We performed both an adjusted correlation analysis based on methylation residuals ( $r_{resid}$ ), which removed covariate effects (see details in Methods section) and an unadjusted correlation analysis based on methylation beta values ( $r_{beta}$ ). Among the significant individual CpGs and CpGs mapped within the DMRs, only eight CpGs showed significant brain-to-blood associations in both adjusted and unadjusted analyses ( $FDR_{beta} < 0.05$ ,  $FDR_{resid} < 0.05$ ; Table S7 in supporting information). All of these CpGs were located in DMRs, and six out eight CpGs showed significant positive brain-to-blood correlations. Notably, the three CpGs with the most significant brain-to-blood correlations ( $r_{beta}$ : 0.821 to 0.851;  $FDR_{beta}$   $3.52 \times 10^{-16}$  to  $6.02 \times 10^{-19}$ ) are located on the *ZNF696* gene, which encodes a zinc finger protein involved in transcriptional regulation (Figure S7 in supporting information).

### 3.5 | Correlation and overlap with genetic risk loci

We identified mQTLs by comparing our dementia-associated CpGs to blood mQTLs from the GoDMC database.<sup>42</sup> Among the 44 significant CpGs (Table S3) and the 233 CpGs located in significant DMRs (Table S4), 96 CpGs had 20974 mQTLs in cis and 12 CpGs had 1464 mQTLs in trans in the blood (Table S8 in supporting information).

Next, we evaluated if the mQTLs overlapped with genetic risk loci implicated in dementia, by comparing them to the genetic variants nominated in a recent ADRD meta-analysis.<sup>43</sup> We found that

while no mQTLs overlapped with the genome-wide significant loci, 272 SNPs overlapped with genetic variants reaching a suggestive genome-wide significance threshold at  $p < 10^{-5}$  (Table S9 in supporting information).

Given the observed overlap between the mQTLs and ADRD genetic risk loci, we next sought to determine whether the association signals at these loci (variant to CpG methylation levels and variant to clinical ADRD status) were due to a single shared causal variant or distinct causal variants close to each other. To this end, we performed a co-localization analysis using the method described by Giambartolomei et al.<sup>50</sup> The results of this co-localization analysis strongly suggested<sup>51</sup> (i.e.,  $PP3+PP4 > 0.90$ ,  $PP4 > 0.8$  and  $PP4/PP3 > 5$ ) that nine genomic regions included a single causal variant common to both phenotypes (i.e., ADRD status and CpG methylation levels). These causal variants are located in the *IL34*, *CCR5AS* genes, and the human leukocyte antigen (HLA) intergenic regions (Table S10 in supporting information).

### 3.6 | Sensitivity analyses

A growing body of recent research suggests that various lifestyle factors, such as smoking, may contribute to dementia.<sup>52,53</sup> Meanwhile, recent studies also reported that DNAm is influenced by lifestyle risk factors.<sup>54-59</sup> We investigated whether any of the significant CpGs were also associated with dementia risk factors collected by the FHS, including APOE, diabetes status, hypertension, years of education, body mass index (BMI), and smoking. We found that among the 271 dementia-associated CpGs (44 significant individual CpGs, 233 CpGs located in significant DMRs, and 6 overlapping CpGs), 43 CpGs are associated with number of APOE  $\epsilon$ 4 alleles, 28 CpGs are associated with smoking status, and 6 CpGs are associated with years of education. Moreover, 13, 18, and 7 CpGs are associated with BMI, diabetes, and hypertension status, respectively (Table S11 in supporting information).

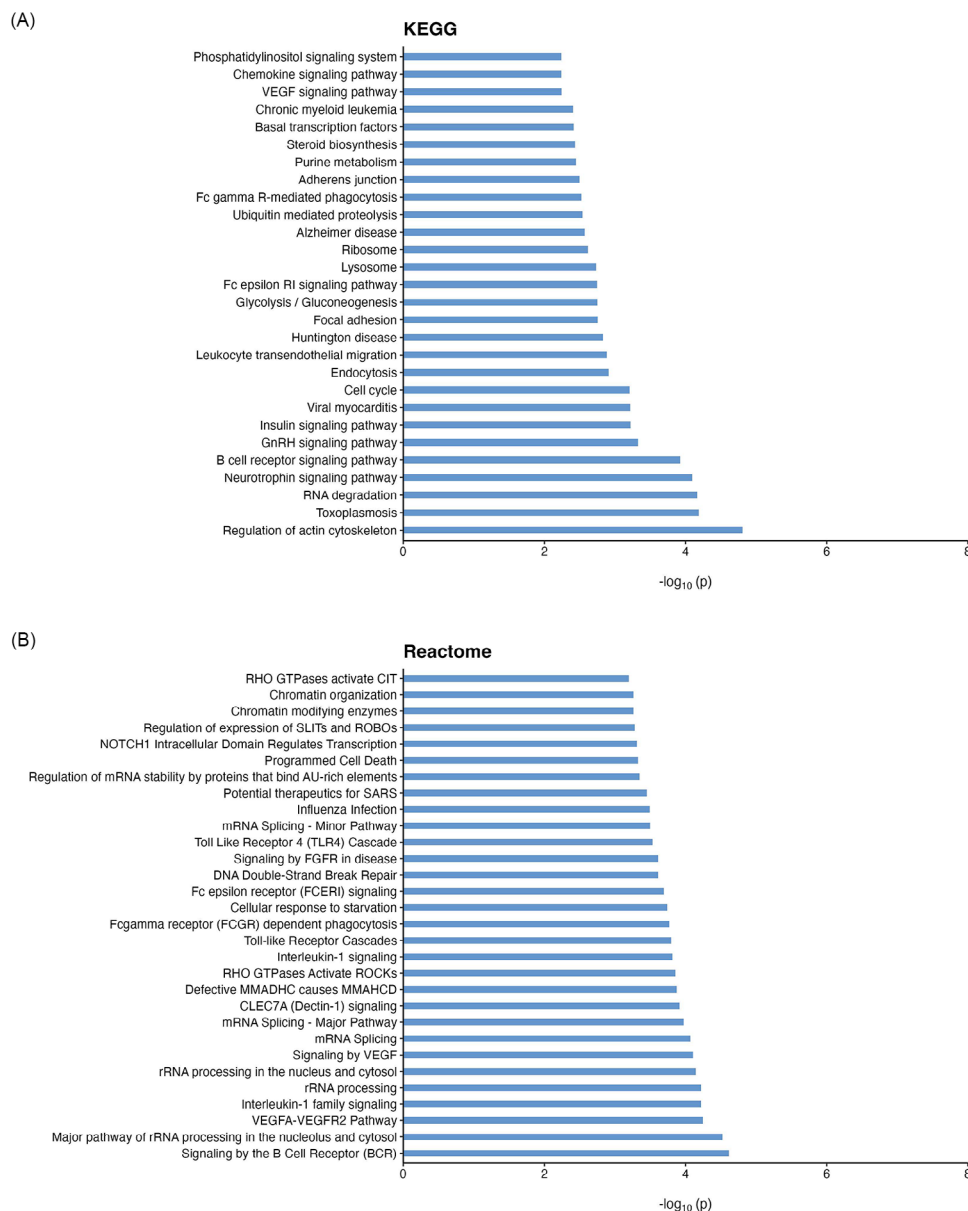


**FIGURE 2** Significant KEGG (A) and Reactome (B) pathways enriched with dementia-associated CpGs at FDR less than 0.05. FDR, false discovery rate; KEGG, Kyoto Encyclopedia of Genes and Genomes.

To evaluate the confounding effects of these risk factors, we reanalyzed the FHS9 dataset and performed a sensitivity analysis of the dementia-associated CpGs, by additionally adjusting for the significant risk factors they were associated with in the Cox regression model. Table S12 in supporting information shows the estimated HRs for all dementia-associated CpGs based on the original model and expanded model are very similar. Moreover, the  $p$  values for the significant individual CpGs ranged from  $1.20 \times 10^{-7}$  to  $4.02 \times 10^{-3}$  in the original model and ranged from  $2.20 \times 10^{-7}$  to 0.0135 in the expanded model, indicating these CpGs are associated with dementia relatively independent of the covariate factors. Given the importance of smoking as a confounding factor for DNAm studies, we also repeated the meta-analysis by additionally including smoking history as a covariate variable. Table S13 in supporting information shows that all 44 dementia-associated

CpGs from Table S3 remained highly significant, with meta-analysis  $p$  values ranging from  $1.79 \times 10^{-8}$  to  $2.15 \times 10^{-5}$ , corroborating the above results.

A second sensitivity analysis was performed to evaluate the impact of family structure in the FHS9 dataset on our analysis results. To this end, we estimated the ICC for the dementia-associated CpGs, by comparing between-family variance to the total variance, which is the sum of between-family variance and within-family variance. Our results showed that for the 271 dementia-associated CpGs, the ICC values ranged from 0 to 0.149 (Table S14 in supporting information), indicating that within-family variance is relatively large compared to between-family variance in DNAm at these CpGs.

In addition, we also performed an additional analysis using mixed-effects Cox models that accounted for family relationships with a

kinship matrix computed from pedigree information. Notably, the  $p$  values for the 44 dementia-associated individual CpGs ranged from  $2.29 \times 10^{-9}$  to  $6.02 \times 10^{-3}$  in the original model, and from  $7.51 \times 10^{-8}$  to  $6.02 \times 10^{-3}$  in the mixed effects Cox model. Table S15 in supporting information shows the HRs and  $p$  values from the mixed effects Cox model are very similar to those from the original Cox model, indicating that our results are robust to family structure in the FHS9 dataset.

In a third sensitivity analysis, we excluded CU subjects with strong biomarker evidence for AD and short follow-up durations. These individuals are at a higher risk of progressing to dementia but may have incomplete data due to the limited follow-up period, which could introduce bias into the analysis. The FHS9 dataset includes plasma total tau measurements, while the ADNI dataset provides cerebrospinal fluid phosphorylated tau (p-tau)181 levels. Given the lack of consensus on specific cutoff values for AD biomarkers, we excluded subjects with tau biomarker levels in the highest quartile and follow-up times in the lowest quartile (i.e.,  $\leq 3$  years). Table S16 in supporting information shows that the meta-analysis  $p$  values for all 44 CpGs remained highly significant, ranging from  $4.41 \times 10^{-8}$  to  $1.14 \times 10^{-5}$ , after excluding these high-risk subjects.

To evaluate the robustness of our DMR analysis results, we performed an additional DMR analysis on the genomic regions defined by the 44 significant DMRs listed in Table S4, using an alternative approach, using the coMethDMR software.<sup>46</sup> Specifically, within each of these 44 genomic regions, we first identified co-methylated and DMRs associated with incident dementia, adjusting for age, sex, and blood cell-type composition for each dataset separately. We then combined the dataset-specific  $p$  values for each genomic region using an inverse-variance fixed-effects meta-analysis model. Our findings indicated that, among the 44 significant DMRs identified by comb-p, the majority (36 DMRs, 81.8%) were significantly associated with incident dementia using coMethDMR at a 5% FDR (Table S17 in supporting information). Additionally, all 36 corroborated DMRs showed the same direction of effect in the coMethDMR method as in the comb-p method.

### 3.7 | Validation of dementia-associated CpGs in independent datasets

To validate our findings, we compared our dementia-associated CpGs and DMRs to those identified in previous studies using our recently developed MIAMI-AD database.<sup>60</sup> Our comparison revealed that 17 of the 44 significant individual CpGs (38.6%) overlapped with significant findings in previous research, with consistent direction of change (Table S18 in supporting information). Among them, results for nine CpGs were from independent cohorts other than FHS and ADNI. These nine CpGs are located in the promoter regions of the *SLCO3A1*, *MUT*, and *WDR75* genes, and intergenic regions. Similarly, among the 227 CpGs located in DMRs, 65 CpGs were supported by previous research, also showing the same direction of effect. Among them, 51 CpGs located in 18 DMRs reached nominal significance with the expected direction of change in external cohorts other than ADNI and FHS.

These 18 DMRs were located in the promoter regions of the *ACY3*, *ARMC5*, *CCR5*, *GET4*, *GLRX*, *IRAX4*, *KIF16B*, *LRR59*, *C6orf25*, *MMACHC*, *HES5*, *PCTP*, *VAV1*, *ZMAT2*, and *ZNF696* genes, and intergenic regions.

### 3.8 | Out-of-sample validation demonstrated an MRS predicted dementia progression

To evaluate the feasibility of using dementia-associated DNAm for predicting disease progression, we developed an MRS score based on significant individual CpGs from the FHS9 dataset and assessed its ability to predict dementia progression in the ADNI dataset.

First, using the FHS9 dataset, we fitted a ridge regression model with time to dementia as the outcome and methylation  $M$  values of 151 CpGs that achieved  $p$  value  $< 10^{-5}$  in the FHS9 dataset (using the model described above in section 2.3) as predictors. Ridge regression reduces model variance by imposing a penalty on the size of the coefficients, leading to more stable and generalizable predictions. The estimated coefficients (i.e., weights) from ridge regression for the 151 CpGs ranged from  $-0.894$  to  $0.997$ , with positive weights assigned to 105 CpGs and negative weights to 46 CpGs (Table S19 in supporting information). Notably, for all 151 CpGs, the directions of these weights were consistent with the estimated effect sizes from univariate Cox regression models that included each CpG individually. Moreover, the weights from ridge regression were significantly correlated with the estimated effect sizes from the univariate Cox regression models (Spearman correlation =  $0.653$ ,  $p$  value  $< 2.2 \times 10^{-16}$ ), supporting the robustness of the directionality of DNAm at these CpGs.

We next performed an out-of-sample validation of the MRS, a weighted sum of methylation  $M$  values of the 151 CpGs, using an external dataset from the ADNI study, which included 538 subjects with available DNAm data and follow-up visit information (Table S20 in supporting information). For each subject, we analyzed the earliest available (baseline) DNAm sample and additionally required the subjects to be CU or MCI at that time. These subjects were followed for an average of  $5.39 \pm 2.94$  years, with follow-up durations ranging from 0.44 to 11.71 years. By their last visit, 64 (30.0%) CU subjects had progressed to MCI or dementia, while 131 (40.3%) of the MCI subjects had progressed to dementia. Notably, the majority of these subjects (182 out of 195 subjects, 93.3%) who progressed to MCI or dementia did so due to AD.

For each of these 538 subjects, we computed MRS scores using DNAm data from their baseline visit and evaluated their association with disease progression (i.e., CU to MCI/dementia, MCI to dementia) using the Cox regression model. The MRS was computed by summing the methylation  $M$  values of the 151 CpGs weighted by their coefficients estimated from FHS9 using ridge regression model. Table 4 shows that after adjusting for age, sex, *APOE*  $\epsilon 4$  status, years of education, baseline diagnosis, and baseline MMSE score, the MRS was significantly associated with progression to the next disease stage (estimate =  $0.142$ ,  $p$  value =  $0.041$ ). Figure 3 shows survival probabilities over time for subjects in the highest and lowest MRS quartiles. Notably, while survival probability decreases in both groups, the group

**TABLE 4** Results from Cox regression model evaluating the association between MRS and disease progression (CU to MCI/dementia, MCI to dementia) in 538 subjects, adjusted for age, sex, APOE  $\epsilon 4$  status, baseline diagnosis, MMSE, and education using ADNI dataset.

Characteristic	Coefficient	HR (95% CI)	p value
MRS	0.142	1.152 (1.006,1.32)	0.041
Age, years	0.066	1.068 (1.047,1.091)	$3.76 \times 10^{-10}$
Male	0.062	1.064 (0.786,1.44)	0.690
<b>Baseline diagnosis</b>			
CU		1 [Reference]	
MCI	0.494	1.639 (1.177,2.281)	$3.44 \times 10^{-3}$
APOE $\epsilon 4$ allele	0.646	1.907 (1.531,2.376)	$8.58 \times 10^{-9}$
MMSE	-0.180	0.835 (0.762,0.916)	$1.26 \times 10^{-4}$
Education, years	-0.002	0.998 (0.942,1.058)	0.949

Note: Significant association was observed for MRS (estimate = 0.142, p-value = 0.0413), indicating higher MRS increases risk.

Abbreviations: APOE, apolipoprotein E; CI, confidence interval; CU, cognitively unimpaired; HR, hazard ratio; MCI, mild cognitive impairment; MMSE, Mini-Mental State Examination; MRS, methylation risk score.

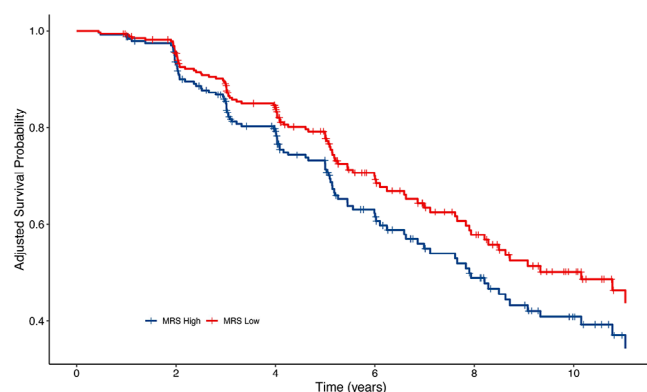


**FIGURE 3** Adjusted Kaplan-Meier curves for dementia progression (CU to MCI/dementia, or MCI to dementia) among subjects in the highest and lowest quartiles of baseline MRS scores in the ADNI cohort. The survival probability decreases in both groups over time. Moreover, the group in the lowest MRS quartile consistently shows a higher survival probability, indicating a lower risk for dementia progression. These results are adjusted for age, sex, APOE  $\epsilon 4$ , years of education, baseline diagnosis, and baseline MMSE score. ADNI, Alzheimer's Disease Neuroimaging Initiative; APOE, apolipoprotein E; CU, cognitively unimpaired; MCI, mild cognitive impairment; MMSE, Mini-Mental State Examination; MRS, methylation risk score.

with low MRS consistently shows a higher survival probability, indicating lower risk of dementia progression. Similarly, when the analysis was limited to dementia due to AD using the same model, the MRS remained significant (estimate = 0.165, p value = 0.0206; Table S21 in supporting information) and the survival probabilities showed similar trends (Figure S8 in supporting information).

## 4 | DISCUSSION

We performed a comprehensive analysis of > 1000 blood samples to identify DNAm associated with incident dementia in two longitudinal studies. After correcting for multiple comparisons, we identified 44 CpGs and 44 DMRs significantly associated with dementia risk (Tables S3 and S4). Comparing these significant DNAm differences to findings from previous cross-sectional studies, we found that about 40% of the significant CpGs and DMRs overlapped with previous results. While differences in sample characteristics, the specific arrays used, and the statistical models applied may contribute to this discrepancy, our findings also suggest that some DNAm differences observed in cross-sectional studies could be due to reverse causation of the disease. The novel DNAm differences discovered in this study highlighted the importance of using a longitudinal design to identify DNAm changes with a temporal relationship to the disease.

To better understand the genetic influences on dementia-associated DNAm, we leveraged the GoDMC database, which includes blood mQTLs computed from 32,851 independent subjects.<sup>42</sup> Consistent with previous observations that genetic influences on DNAm in the blood are widespread,<sup>61</sup> we found that about 40% (99 out of 271 CpGs) of our dementia-associated CpGs are associated with mQTLs. This is similar to findings by Min et al., who estimated that genetic variants influence about 45% of DNAm sites on the Illumina array.<sup>42</sup> To prioritize potential regulatory variants causally involved in dementia, we performed a co-localization analysis of association signals from two independent studies: the mQTLs of dementia-associated DNAm identified in this study and genetic risk loci implicated in a recent ADRD genome-wide association study.<sup>43</sup> The co-localization analysis revealed that a subset of CpGs are influenced by mQTLs (i.e., SNPs) linked to ADRD risk. The significant co-localization signals at these loci provided strong support that ADRD and CpG methylation are associated with the same causal genetic variant. These nominated causal genetic variants are located on the *IL34* and *CCR5AS* genes, and the HLA intergenic region, all of which are involved in neuroinflammatory responses relevant to dementia. Future studies using multi-omics data, including genetic variants, DNAm, and dementia outcomes, are needed to thoroughly investigate and confirm whether the genetic associations with AD at these loci are mediated by methylation modifications at nearby CpG sites. Alternatively, these DNAm differences might simply be peripheral markers of indirect systemic effects reflecting the underlying AD-related pathology. Given that the primary pathology of AD occurs in brain tissue, future studies of mQTLs and co-localization in both brain and blood samples, especially cell-type specific studies, will provide additional insights into the genetic regulatory mechanisms by which the dementia-associated loci may influence DNAm to affect disease risk.

Compared to gene expression and proteins, methylated DNA is relatively stable and can be easily detected, thus serving as an excellent source of biomarkers.<sup>62</sup> Recently, a number of blood-based AD biomarkers, such as the high-performing plasma p-tau217, have been developed and shown to be significantly associated with the future development of AD dementia in subjects with MCI.<sup>63</sup> However,

autopsy studies have observed a discordance between neuropathological burden and cognitive performance.<sup>64</sup> These studies have revealed that among CU subjects, about 25% exhibit amyloid abnormalities in the brain that meet the neuropathological criteria for AD.<sup>65,66</sup> Similarly, current pathology biomarkers do not completely predict subsequent cognitive impairment in asymptomatic individuals. For example, in a recent study by Ossenkoppele et al., among CU subjects identified with both amyloid and tau pathology (A+T+), as measured by amyloid positron emission tomography (PET) and tau PET, which indicates a high likelihood of progression to MCI or AD, a substantial proportion ( $\approx 36\%$ , 40 out of 111) remained CU after an average of 42 months of follow-up.<sup>67</sup>

Cognitive resilience (CR) refers to the adaptability of an individual to brain changes due to disease, injury, or normal aging.<sup>68,69</sup> Higher CR has been associated with a lower risk of progression to clinical AD and a slower rate of cognitive decline.<sup>70</sup> Lifestyle factors such as engaging in physical activity and following the MIND diet, which have been shown to be associated with DNAm, play important roles in promoting CR and delaying cognitive decline.<sup>71–74</sup> Therefore, DNAm holds great promise as a complementary biomarker to existing pathology biomarkers, facilitating a more precise determination of dementia risk.

The strengths of this study include the longitudinal design of the FHS and ADNI studies, which allowed us to identify DNAm associated with incident dementia. In both studies, dementia status was adjudicated by a team of experts. The DNAm samples in both ADNI and FHS9 studies were measured using Illumina EPIC arrays, which provide improved coverage of regulatory elements<sup>75</sup> and were recently shown to generate more reliable DNAm levels than the older 450k arrays.<sup>76</sup> To reduce false positives, we adjusted potential confounding effects such as age, sex, estimated major immune cell-type proportions, and corrected for batch effects and inflation.<sup>33</sup> Moreover, we used stringent criteria to select our significant CpGs and DMRs. For significant individual CpGs, we required consistent directional effects and nominal significance in both cohorts. For DMRs, we required all CpGs within the DMR to have consistent directional effects. We evaluated the sensitivity of our results to major risk factors of dementia, some of which also correlated with DNAm. We found that all of our 44 dementia-associated CpGs remained significant, indicating their association with dementia is independent of the risk factors. We also estimated ICCs and performed additional analyses accounting for family relationships in FHS9 using a kinship matrix. The results of this analysis showed our findings are robust to family structure in the FHS9 dataset. Finally, and importantly, we showed that the MRS developed using the Framingham study dataset is significantly associated with progression to MCI or dementia in the ADNI dataset, even after accounting for age, sex, APOE  $\epsilon 4$ , years of education, baseline diagnosis, and baseline MMSE score. Recently, Koetsier et al. also developed a DNAm-based risk score that successfully predicted future cognitive impairment in independent AD and Parkinson's disease datasets, by leveraging DNAm associated with 14 modifiable and non-modifiable dementia risk factors.<sup>77</sup> Our study, which identified DNAm directly associated with incident dementia, and the study by Koetsier et al., which discovered DNAm associated with

dementia risk factors, provided complementary approaches for discovering risk variants for dementia. Together, the results of our study and theirs demonstrate that DNAm is a plausible predictive biomarker that precedes dementia onset.

This study has several limitations. First, we analyzed bulk blood DNAm samples that contain a mixture of cell types. To reduce confounding effects due to cellular heterogeneity, we included estimated cell-type proportions as covariates in all our analyses. Future studies using single-cell technology could provide more detailed insights into the specific cell types affected by the dementia-associated DNAm differences identified here. However, single-cell methylomic technologies currently face significant practical challenges. These methods typically involve high costs, complex data processing, and require substantial technical expertise, which can limit their scalability, especially for large, complex disease cohorts like those studied in ADRD research. Moreover, the heterogeneity inherent in ADRD complicates the application of single-cell approaches, as large sample sizes across diverse cell populations are needed to capture meaningful biological variability.

Second, an interesting observation is the distribution of hypermethylated CpGs and DMRs, in which approximately half (21 out of 44) of the FDR-significant CpGs were hypermethylated, compared to three quarters (35 out of 44) of the identified DMRs. This discrepancy may reflect potential biases inherent in array-based technology, which includes a higher density of probes within promoter regions, areas where DMRs are more likely to be detected. Such biases could have contributed to the observed higher proportion of hypermethylated DMRs. The use of sequencing-based technologies in future studies would help to overcome these biases by offering more comprehensive and unbiased coverage of the methylome.

Third, to help increase sample size, we used a broad definition of dementia to identify DNAm signatures, which might have diluted association signals due to the heterogeneity among various dementia subtypes. However, the majority of dementia events in our study were attributed to AD. In the FHS9 dataset, 32 of 42 (76.2%) dementia events were due to AD, and in the ADNI dataset, 15 of 18 (83.3%) dementia events were due to AD. When we repeated the meta-analysis of FHS9 and ADNI datasets using the same models but replacing time to incident dementia with time to AD dementia, the results were very similar. In particular, the meta-analysis *p* value for all 44 CpGs in Table S3 remained highly significant, ranging from  $5.26 \times 10^{-8}$  to  $6.85 \times 10^{-3}$  (Table S22 in supporting information). Moreover, the MRS score developed using the FHS9 dataset, with time to dementia as the outcome variable, validated well in the ADNI dataset, and was significantly associated with progression to MCI or dementia due to AD, even after adjusting for covariate variables (Table S21 and Figure S8). Finally, the insidious onset of dementia might lead to underreporting, with some subjects reaching dementia status before their recorded onset date. These cases could dilute the association signals between DNAm and incident dementia in our study, making our meta-analysis results conservative. Therefore, a sensitive and objective biomarker, such as DNAm that can be easily quantified, is urgently needed to help improve surveillance of incident dementia.



In summary, we identified numerous DNAm differences consistently associated with incident dementia in a meta-analysis of two longitudinal cohorts. Our integrative analysis of blood DNAm with gene expression, genetic variants, and brain DNAm data highlights the central role of neuroinflammation and early processes such as metabolic dysfunction in dementia. Importantly, our out-of-sample validation demonstrated that MRSs based on dementia-associated DNAm predicted future cognitive decline in an independent dataset, even after accounting for covariate variables, supporting blood DNAm as a potential objective biomarker for identifying individuals at higher risk for dementia. Future studies that validate our findings in larger and more diverse community-based cohorts are warranted.

## ACKNOWLEDGMENTS

The authors would like to thank Dr. Rhoda Au and her team for their valuable assistance in enhancing our understanding of the FHS dataset. Data collection and sharing for the ADNI dataset was funded by the ADNI (National Institutes of Health Grant U01 AG024904) and DOD ADNI (Department of Defense award number W81XWH-12-2-0012). ADNI is funded by the National Institute on Aging, the National Institute of Biomedical Imaging and Bioengineering, and through generous contributions from the following: AbbVie; Alzheimer's Association; Alzheimer's Drug Discovery Foundation; Araclon Biotech; BioClinica, Inc.; Biogen; Bristol-Myers Squibb Company; CereSpir, Inc.; Cogstate; Eisai Inc.; Elan Pharmaceuticals, Inc.; Eli Lilly and Company; EuroImmun; F. Hoffmann-La Roche Ltd and its affiliated company Genentech, Inc.; Fujirebio; GE Healthcare; IXICO Ltd.; Janssen Alzheimer Immunotherapy Research & Development, LLC; Johnson & Johnson Pharmaceutical Research & Development LLC; Lumosity; Lundbeck; Merck & Co., Inc.; Meso Scale Diagnostics, LLC; NeuroRx Research; Neurotrack Technologies; Novartis Pharmaceuticals Corporation; Pfizer Inc.; Piramal Imaging; Servier; Takeda Pharmaceutical Company; and Transition Therapeutics. The Canadian Institutes of Health Research is providing funds to support ADNI clinical sites in Canada. Private sector contributions are facilitated by the Foundation for the National Institutes of Health ([www.fnih.org](http://www.fnih.org)). The grantee organization is the Northern California Institute for Research and Education, and the study is coordinated by the Alzheimer's Therapeutic Research Institute at the University of Southern California. ADNI data are disseminated by the Laboratory for Neuro Imaging at the University of Southern California. This research was supported by US National Institutes of Health grants R61NS135587 (L.W.), RF1NS128145 (L.W.), and R01AG062634 (E.R.M, B.W.K., L.W.).

## CONFLICT OF INTEREST STATEMENT

The authors declare no conflicts of interest. Author disclosures are available in the [supporting information](#).

## CONSENT STATEMENT

The ADNI and FHS were approved by the institutional review boards of all participating institutions. Written informed consent was obtained from all the participants or their authorized representatives.

## REFERENCES

- Hurd MD, Martorell P, Delavande A, Mullen KJ, Langa KM. Monetary costs of dementia in the United States. *N Engl J Med*. 2013;368:1326-1334.
- Ty D, Ahuja R. Projected Prevalence and Cost of Dementia: 2022. Update 2022. Accessed November 26, 2024. [https://milkeninstitute.org/sites/default/files/2022-11/Projected%20Prevalence%20and%20Cost%20of%20Dementia%202022%20Update\\_Highlights\\_FINAL\\_Nov.pdf](https://milkeninstitute.org/sites/default/files/2022-11/Projected%20Prevalence%20and%20Cost%20of%20Dementia%202022%20Update_Highlights_FINAL_Nov.pdf)
- Zissimopoulos J, Crimmins E, St Clair P. The value of delaying Alzheimer's disease onset. *Forum Health Econ Policy*. 2014;18:25-39.
- Zhang L, Silva TC, Young JI, et al. Epigenome-wide meta-analysis of DNA methylation differences in prefrontal cortex implicates the immune processes in Alzheimer's disease. *Nat Commun*. 2020;11:6114.
- Zhang L, Young JI, Gomez L, et al. Sex-specific DNA methylation differences in Alzheimer's disease pathology. *Acta Neuropathol Commun*. 2021;9:77.
- Silva TC, Zhang W, Young JI, et al. Distinct sex-specific DNA methylation differences in Alzheimer's disease. *Alzheimers Res Ther*. 2022;14:133.
- Silva TC, Young JI, Zhang L et al. Cross-tissue analysis of blood and brain epigenome-wide association studies in Alzheimer's disease. *Nat Commun*. 2022;13:4852.
- De Jager PL, Srivastava G, Lunnon K, et al. Alzheimer's disease: early alterations in brain DNA methylation at ANK1, BIN1, RHBDL2 and other loci. *Nat Neurosci*. 2014;17:1156-1163.
- Lunnon K, Smith R, Hannon E, et al. Methyloomic profiling implicates cortical deregulation of ANK1 in Alzheimer's disease. *Nat Neurosci*. 2014;17:1164-1170.
- Smith RG, Hannon E, De Jager PL, et al. Elevated DNA methylation across a 48-kb region spanning the HOXA gene cluster is associated with Alzheimer's disease neuropathology. *Alzheimers Dement*. 2018;14:1580-1588.
- Smith RG, Pishva E, Shireby G, et al. A meta-analysis of epigenome-wide association studies in Alzheimer's disease highlights novel differentially methylated loci across cortex. *Nat Commun*. 2021;12:3517.
- Fransquet PD, Lacaze P, Saffery R, McNeil J, Woods R, Ryan J. Blood DNA methylation as a potential biomarker of dementia: a systematic review. *Alzheimers Dement*. 2018;14:81-103.
- Kobayashi N, Shinagawa S, Niimura H, et al. Increased blood COASY DNA methylation levels a potential biomarker for early pathology of Alzheimer's disease. *Sci Rep*. 2020;10:12217.
- Roubroeks JAY, Smith AR, Smith RG, et al. An epigenome-wide association study of Alzheimer's disease blood highlights robust DNA hypermethylation in the HOXB6 gene. *Neurobiol Aging*. 2020;95:26-45.
- Fransquet PD, Lacaze P, Saffery R, et al. DNA methylation analysis of candidate genes associated with dementia in peripheral blood. *Epigenomics*. 2020;12:2109-2123.
- Madrid A, Hogan KJ, Papale LA, et al. DNA Hypomethylation in blood links B3GALT4 and ZADH2 to Alzheimer's disease. *J Alzheimers Dis*. 2018;66:927-934.
- Mitsumori R, Sakaguchi K, Shigemizu D, et al. Lower DNA methylation levels in CpG island shores of CR1, CLU, and PICALM in the blood of Japanese Alzheimer's disease patients. *PLoS One*. 2020;15:e0239196.
- Roubroeks JAY, Smith RG, van den Hove DLA, Lunnon K. Epigenetics and DNA methylomic profiling in Alzheimer's disease and other neurodegenerative diseases. *J Neurochem*. 2017;143:158-170.
- Fransquet PD, Lacaze P, Saffery R, et al. Blood DNA methylation signatures to detect dementia prior to overt clinical symptoms. *Alzheimers Dement (Amst)*. 2020;12:e12056.
- Li QS, Vasanthakumar A, Davis JW, et al. Association of peripheral blood DNA methylation level with Alzheimer's disease progression. *Clin Epigenetics*. 2021;13:191.

21. Schafer Hackenhaar F, Josefsson M, Nordin Adolfsson A, et al. Sixteen-year longitudinal evaluation of blood-based DNA methylation biomarkers for early prediction of Alzheimer's disease. *J Alzheimers Dis*. 2023;94:1443-1464.
22. Giannini LAA, Boers RG, van der Ende EL, et al. Distinctive cell-free DNA methylation characterizes presymptomatic genetic frontotemporal dementia. *Ann Clin Transl Neurol*. 2024;11:744-756.
23. Andersson C, Johnson AD, Benjamin EJ, Levy D, Vasan RS. 70-year legacy of the Framingham Heart Study. *Nat Rev Cardiol*. 2019;16:687-698.
24. Satizabal C, Beiser AS, Seshadri S. Incidence of dementia over three decades in the Framingham Heart Study. *N Engl J Med*. 2016;375:93-94.
25. Veitch DP, Weiner MW, Aisen PS, et al. Understanding disease progression and improving Alzheimer's disease clinical trials: recent highlights from the Alzheimer's disease neuroimaging initiative. *Alzheimers Dement*. 2019;15:106-152.
26. Kim BH, Vasanthakumar A, Li QS, et al. Harnessing peripheral DNA methylation differences in the Alzheimer's Disease Neuroimaging Initiative (ADNI) to reveal novel biomarkers of disease. *Clin Epigenetics*. 2020;12:84.
27. Chen YA, Lemire M, Choufani S, et al. Discovery of cross-reactive probes and polymorphic CpGs in the Illumina Infinium HumanMethylation450 microarray. *Epigenetics*. 2013;8:203-209.
28. Pidsley RY, Wong CC, Volta M, Lunnon K, Mill J, Schalkwyk LC. A data-driven approach to preprocessing Illumina 450K methylation array data. *BMC Genomics*. 2013;14:293.
29. Teschendorff AE, Breeze CE, Zheng SC, Beck S. A comparison of reference-based algorithms for correcting cell-type heterogeneity in Epigenome-Wide Association Studies. *BMC Bioinformatics*. 2017;18:105.
30. Nabais MF, Laws SM, Lin T, et al. Meta-analysis of genome-wide DNA methylation identifies shared associations across neurodegenerative disorders. *Genome Biol*. 2021;22:90.
31. Akulenko R, Merl M, Helms V. BEclear: batch effect detection and adjustment in DNA methylation data. *PLoS One*. 2016;11:e0159921.
32. Delvin B, Roeder K. Genomic control for association studies. *Biometrics*. 1999;55:997-1004.
33. van Iterson M, van Zwet EW, Consortium B, Heijmans BT. Controlling bias and inflation in epigenome- and transcriptome-wide association studies using the empirical null distribution. *Genome Biol*. 2017;18:19.
34. Rice K, Higgins JPT, Lumley T. A re-evaluation of fixed effect(s) meta-analysis. *J R Statist Soc A*. 2018;181:205-227.
35. Pedersen BS, Schwartz DA, Yang IV, Kechris KJ. Comb-p: software for combining, analyzing, grouping and correcting spatially correlated P-values. *Bioinformatics*. 2012;28:2986-2988.
36. Mallik S, Odom GJ, Gao Z, Gomez L, Chen X, Wang L. An evaluation of supervised methods for identifying differentially methylated regions in Illumina methylation arrays. *Brief Bioinform*. 2019;20:2224-2235.
37. McLean CY, Bristol D, Hiller M, et al. GREAT improves functional interpretation of cis-regulatory regions. *Nat Biotechnol*. 2010;28:495-501.
38. Nasser J, Bergman DT, Fulco CP, et al. Genome-wide enhancer maps link risk variants to disease genes. *Nature*. 2021;593:238-243.
39. Ren X, Kuan PF. methylGSA: a Bioconductor package and Shiny app for DNA methylation data length bias adjustment in gene set testing. *Bioinformatics*. 2019;35:1958-1959.
40. Subramanian A, Tamayo P, Mootha VK, et al. Gene set enrichment analysis: a knowledge-based approach for interpreting genome-wide expression profiles. *Proc Natl Acad Sci U S A*. 2005;102:15545-15550.
41. Yao C, Joehanes R, Wilson R, et al. Epigenome-wide association study of whole blood gene expression in Framingham Heart Study participants provides molecular insight into the potential role of CHRNA5 in cigarette smoking-related lung diseases. *Clin Epigenetics*. 2021;13:60.
42. Min JL, Hemani G, Hannon E, et al. Genomic and phenotypic insights from an atlas of genetic effects on DNA methylation. *Nat Genet*. 2021;53:1311-1321.
43. Bellenguez C, Küçükali F, Jansen IE, et al. New insights into the genetic etiology of Alzheimer's disease and related dementias. *Nat Genet*. 2022;54:412-436.
44. Hannon E, Lunnon K, Schalkwyk L, Mill J. Interindividual methylomic variation across blood, cortex, and cerebellum: implications for epigenetic studies of neurological and neuropsychiatric phenotypes. *Epigenetics*. 2015;10:1024-1032.
45. Therneau T. *coxme: Mixed Effects Cox Models (Version 2.2-22)* [R package] Comprehensive R Archive Network (CRAN).
46. Gomez L, Odom GJ, Young JI, et al. coMethDMR: accurate identification of co-methylated and differentially methylated regions in epigenome-wide association studies with continuous phenotypes. *Nucleic Acids Res*. 2019;47:e98.
47. Mukherjee S, Erickson H, Bastia D. Enhancer-origin interaction in plasmid R6K involves a DNA loop mediated by initiator protein. *Cell*. 1988;52:375-383.
48. Craft S. The role of metabolic disorders in Alzheimer disease and vascular dementia: two roads converged. *Arch Neurol*. 2009;66:300-305.
49. Ezkurdia A, Ramirez MJ, Solas M. Metabolic syndrome as a risk factor for Alzheimer's disease: a focus on insulin resistance. *Int J Mol Sci*. 2023;24.
50. Giambartolomei C, Vukcevic D, Schadt EE, et al. Bayesian test for colocalisation between pairs of genetic association studies using summary statistics. *PLoS Genet*. 2014;10:e1004383.
51. Guo H, Fortune MD, Burren OS, Schofield E, Todd JA, Wallace C. Integration of disease association and eQTL data using a Bayesian colocalisation approach highlights six candidate causal genes in immune-mediated diseases. *Hum Mol Genet*. 2015;24:3305-3313.
52. Livingston G, Huntley J, Sommerlad A, et al. Dementia prevention, intervention, and care: 2020 report of the Lancet Commission. *Lancet*. 2020;396:413-446.
53. Ranson JM, Rittman T, Hayat S, et al. Modifiable risk factors for dementia and dementia risk profiling. A user manual for Brain Health Services-part 2 of 6. *Alzheimers Res Ther*. 2021;13:169.
54. Walker RM, Bermingham ML, Vaher K, et al. Epigenome-wide analyses identify DNA methylation signatures of dementia risk. *Alzheimers Dement (Amst)*. 2020;12:e12078.
55. Philibert RA, Beach SR, Brody GH. The DNA methylation signature of smoking: an archetype for the identification of biomarkers for behavioral illness. *Nebr Symp Motiv*. 2014;61:109-127.
56. Demura M, Saijoh K. The role of DNA methylation in hypertension. *Adv Exp Med Biol*. 2017;956:583-598.
57. Raciti GA, Desiderio A, Longo M, et al. DNA methylation and type 2 diabetes: novel Biomarkers for risk assessment? *Int J Mol Sci*. 2021;22:11652.
58. Samblas M, Milagro FI, Martinez A. DNA methylation markers in obesity, metabolic syndrome, and weight loss. *Epigenetics*. 2019;14:421-444.
59. Zhao W, Ammous F, Ratliff S, et al. Education and lifestyle factors are associated with DNA methylation clocks in older African Americans. *Int J Environ Res Public Health*. 2019;16.
60. Lukacsovich D, O'Shea D, Huang H, et al. MIAMI-AD (Methylation in Aging and Methylation in AD): an integrative knowledgebase that facilitates explorations of DNA methylation across sex, aging, and Alzheimer's disease. *Database*. 2024;2024:baae061.
61. van Dongen J, Nivard MG, Willemsen G, et al. Genetic and environmental influences interact with age and sex in shaping the human methylome. *Nat Commun*. 2016;7:11115.
62. Mikeska T, Craig JM. DNA methylation biomarkers: cancer and beyond. *Genes (Basel)*. 2014;5:821-864.

63. Hansson O, Blennow K, Zetterberg H, Dage J. Blood biomarkers for Alzheimer's disease in clinical practice and trials. *Nat Aging*. 2023;3:506-519.
64. Boyle PA, Wilson RS, Yu L, et al. Much of late life cognitive decline is not due to common neurodegenerative pathologies. *Ann Neurol*. 2013;74:478-489.
65. Jansen WJ, Janssen O, Tijms BM, et al. Prevalence estimates of amyloid abnormality across the Alzheimer disease clinical spectrum. *JAMA Neurol*. 2022.
66. Ossenkoppele R, Jansen WJ, Rabinovici GD, et al. Prevalence of amyloid PET positivity in dementia syndromes: a meta-analysis. *JAMA*. 2015;313:1939-1949.
67. Ossenkoppele R, Pichet Binette A, Groot C, et al. Amyloid and tau PET-positive cognitively unimpaired individuals are at high risk for future cognitive decline. *Nat Med*. 2022;28:2381-2387.
68. Arenaza-Urquijo EM, Vemuri P. Resistance vs resilience to Alzheimer disease: clarifying terminology for preclinical studies. *Neurology*. 2018;90:695-703.
69. Hohman TJ, McLaren DG, Mormino EC, et al. Asymptomatic Alzheimer disease: defining resilience. *Neurology*. 2016;87:2443-2450.
70. Bocancea DI, van Loenhoud AC, Groot C, Barkhof F, van der Flier WM, Ossenkoppele R. Measuring resilience and resistance in aging and Alzheimer disease using residual methods: a systematic review and meta-analysis. *Neurology*. 2021;97:474-488.
71. Dhana K, James BD, Agarwal P, et al. MIND Diet, common brain pathologies, and cognition in community-dwelling older adults. *J Alzheimers Dis*. 2021;83:683-692.
72. Rabin JS, Klein H, Kirn DR, et al. Associations of physical activity and beta-amyloid with longitudinal cognition and neurodegeneration in clinically normal older adults. *JAMA Neurol*. 2019;76:1203-1210.
73. Ma J, Rebholz CM, Braun KVE, et al. Whole blood DNA methylation signatures of diet are associated with cardiovascular disease risk factors and all-cause mortality. *Circ Genom Precis Med*. 2020;13:e002766.
74. Turner DC, Gorski PP, Maasar MF, et al. DNA methylation across the genome in aged human skeletal muscle tissue and muscle-derived cells: the role of HOX genes and physical activity. *Sci Rep*. 2020;10:15360.
75. Pidsley R, Zotenko E, Peters TJ, et al. Critical evaluation of the Illumina MethylationEPIC BeadChip microarray for whole-genome DNA methylation profiling. *Genome Biol*. 2016;17:208.
76. Zhang W, Young JI, Gomez L, et al. Critical evaluation of the reliability of DNA methylation probes on the Illumina MethylationEPIC v1.0 BeadChip microarrays. *Epigenetics*. 2024;19:2333660.
77. Koetsier J, Cavill R, Reijnders R, et al. Blood-based multivariate methylation risk score for cognitive impairment and dementia. *Alzheimers Dement*. 2024;20:6682-6698.

## SUPPORTING INFORMATION

Additional supporting information can be found online in the Supporting Information section at the end of this article.

**How to cite this article:** Zhang W, Young JI, Gomez L, et al. Blood DNA methylation signature for incident dementia: Evidence from longitudinal cohorts. *Alzheimer's Dement*. 2025;21:e14496. <https://doi.org/10.1002/alz.14496>